Next Sustainability 3 (2024) 100030

Contents lists available at ScienceDirect

Next Sustainability

journal homepage: www.sciencedirect.com/journal/next-sustainability

Research article

Maximizing selectivity and activity in the catalytic reduction of nitrates with formic acid under optimal pH conditions

Fernanda Miranda Zoppas[a,*,1], Nicolás Sacco[a], Thiago Beltrame[b], Faheem Akhter[c], Eduardo Miró[a], Fernanda Albana Marchesini[a]

[a] Institute of Catalysis and Petrochemistry Research (INCAPE-CONICET), Santa Fe, Argentina
[b] Laboratory of Corrosion, Protection and Recycling of Materials LACOR-UFRGS (Federal University of Rio Grande do Sul), Av. Bento Gonçalves, Porto Alegre, RS 9500, Brazil
[c] Department of Chemical Engineering, Quaid-E-Awam University of Engineering, Science & Technology, Nawabshah, Pakistan

ARTICLE INFO

Keywords:
Formic acid
Bimetallic catalyst
Nitrate
Operating parameters
Catalytic reduction

ABSTRACT

This study delves into the catalytic reduction of nitrate in water using a Pd 1(wt%) In 0.25(wt%) catalyst supported on alumina. Investigating the influence of formic acid concentration, pH control, and catalyst characteristics on performance and selectivity, we find that higher formic acid concentrations boost initial reaction rates until saturation, impacting activity. Stoichiometric formic acid concentration strikes the best balance between activity and N_2 selectivity. Comparative studies with hydrogen highlight formic acid's unique role in nitrate reduction. pH control using formic acid ensures full nitrate conversion, highlighting its dual role as a pH regulator and reducing agent. Additionally, the study uncovers a volcano-type behavior and surface properties affecting catalytic activity. Characterization through XPS, XRD, and SEM techniques provides valuable insights into the catalyst's composition and distribution. This comprehensive investigation sheds light on key parameters influencing catalytic nitrate reduction, guiding optimal water treatment processes. The economically advantageous and efficient (Pd, In)-based catalyst emerges as a promising solution for nitrate removal applications, addressing global water contamination challenges.

Introduction

Water contamination with nitrate is a global problem that has already been recognized. According to the World Health Organization (WHO), the established limit for this anion in drinking water is 10 mg/L N-NO_3^-. Among the possible technologies for treating water contaminated with nitrate, catalytic reduction is attractive because it converts nitrate into N_2 and H_2O. This process uses bimetallic catalysts composed of a noble metal (Pd, Ir, Rh, or Pt) and a promoter metal (Cu, Sn, In, Ag, Ni, etc.) [1] and has been used to treat wastewater, such as concentrates from desalination or electrodialysis processes. These effluents are characterized by containing nitrate concentrations between 67 and 361 mg/L N-NO_3^- [2].

Alumina, known for its advantageous properties such as high surface area, thermal stability, and chemical inertness in nitrate reduction [3–5] serves as a widely used support material for catalysts. In the context of global concerns regarding water pollution, our work aligns with the increasing necessity to address environmental issues through catalytic methods, emphasizing the degradation of contaminants in wastewater [6–9].

The mechanism for catalytic reduction of nitrate occurs in two stages: (1) the reduction of NO_3^- to NO_2^-, (2) the reduction of NO_2^- to N_2 or NH_4^+. In turn, the limits of the World Health Organization (WHO) for nitrite and ammonium in drinking water are 0.1 N-mg/L and 1 N-mg/L, respectively. For the first stage, in addition to Pd, a promoter metal (e.g., Cu, Sn, In) is necessary to initiate the reduction of nitrate. For the reduction of nitrites and subsequent intermediates, only the presence of the noble metal, such as Pd or Pt, is required. The most commonly used reducing agent in this reaction is hydrogen; however, recent studies by our group show that organic reducing agents such as formic acid (FA) have promising results [10] for replacing hydrogen in the catalytic process. Due to its chemical characteristics, FA decomposes into H_2 and CO_2 on the surface of noble metals such as Pd, providing the reducing agent in a controlled manner, and CO_2 acts as an *in situ* buffer in the

---

* Corresponding author.
E-mail address: fzoppas@fiq.unl.edu.ar (F.M. Zoppas).
[1] ORCID ID: https://orcid.org/0000-0002-7747-2183

https://doi.org/10.1016/j.nxsust.2024.100030
Received 3 September 2023; Received in revised form 19 February 2024; Accepted 23 February 2024
Available online 1 March 2024

reaction medium through the chemical equilibrium CO_2-bicarbonate [11]. The great advantage of this system is that the generated CO_2 can neutralize the OH^- produced by the reduction of NO_3^-.

Among the bimetallic pairs used, Pd and In are already well-established as a selective and active pair in the reduction of NO_3^- using H_2 as the reducing agent [12,13]. Currently, efforts are being made to replace gaseous H_2 with a safer hydrogen storage system to operate since it is insoluble and needs to be used in excess in nitrate reduction to achieve high catalytic activity. For this reason, formic acid has emerged as an attractive option for catalytic nitrate reduction.

The main parameters that affect the catalytic activity of nitrate reduction, operating in batch mode, include temperature, agitation, pH, catalyst amount, proportion between active phases in the catalytic support, initial concentration of reducing agent, and initial concentration of contaminant. Literature reports some studies that show the behavior of nitrate reduction in aqueous phase using different proportions of active phase [14]. Research on the catalytic reduction of nitrates using formic acid as a reducing agent has been extensively explored, with various studies contributing valuable insights. The catalytic reduction of nitrates is crucial in addressing water pollution issues globally. For instance, the use of $PdAg/SiO_2$-NH_2 catalysts has shown enhanced nitrate reduction performance, leveraging surface modification and efficient electron transfer mechanisms [15]. Another study focused on the reactions of nitrate ions with small organic acids under ultraviolet illumination, revealing a photoinduced process with potential applications in oceans, lakes, and rivers [16]. Catalysts of Pd-In supported on activated carbon fiber were synthesized and evaluated for the removal of nitrogen oxyanions, demonstrating high selectivity to N_2 using formic acid as a reducing agent [17]. Activated carbon fibers coated with Pd and In were employed as structured catalysts, exhibiting efficient decontamination of water containing nitrates with selectivity to gaseous nitrogen exceeding 99% [18].

Moreover, efforts have been made to explore alternative processes for formic acid mineralization from nitrate catalytic reduction effluents. UV-based and electrochemical processes were proposed, with electrochemical oxidation showing the best results in formic acid mineralization and demonstrating resilience to the addition of nitrate [19]. This suggests the potential of electrochemical methods in minimizing energy consumption during formic acid mineralization. Additionally, the development of a water-soluble highly efficient iridium catalyst for chemoselective reduction using formic acid as a reducing agent presents a promising avenue for diverse applications [20]. Similarly, the synthesis of networked Ag/AgPd core/shell nanowires for bifunctional catalysis of nitrate and nitrite removal using formic acid expands the repertoire of catalytic materials for water treatment [21]. Furthermore, catalytic nitrate removal from brines and water with high nitrate concentration using a low noble metal loading catalyst (Pd 1 wt%, In 0.25 wt%) contributes to the understanding of nitrate reduction under different conditions [10]. These comprehensive studies collectively provide valuable information for water environmental control technologies and the development of green synthesis processes [10,15,16,18–21].

In the antecedent investigation [10], the Pd-In bimetallic catalyst's efficacy in reducing nitrate concentrations from brines and water with high nitrate levels was thoroughly examined. The study established the catalyst's performance under diverse conditions, thereby enriching the collective knowledge on water environmental control technologies and green synthesis processes. The success of the Pd 1 wt%, In 0.25 wt% catalyst in nitrate reduction provided a solid foundation for subsequent inquiries. This in-depth exploration significantly contributed to the existing literature on formic acid-mediated catalytic nitrate reduction, underscoring the importance of a meticulous understanding of operational parameters. Building upon these insights, the current study aims to further refine the catalytic process by systematically evaluating various parameters in the catalytic reduction of nitrate, using formic acid as a hydrogen source. The objective is to determine the catalyst's optimal operating conditions for reducing NO_3^-, aiming for the best compromise between catalytic activity and N_2 selectivity. The novelty of this work lies in its comprehensive investigation of the catalytic reduction process using formic acid, examining operational parameters such as pH, and the initial concentration of both the reducing agent and contaminant. This study not only bridges existing gaps in the literature but also emphasizes the careful selection of the synthesis method, aligning with the most suitable approach identified in the initial work. Additionally, it expands the scope of catalytic applications to wastewater, beyond brines, and explores nitrate reduction at lower concentrations, demonstrating the versatility and broader relevance of the catalytic method in water treatment.

Material and methods

Catalyst synthesis

Initially, the alumina support (γ-Al_2O_3 CK300, specific area 180 m^2/g, pore volume 0.5 cm^3/g) was pretreated by calcination at 500°C for 4 h. Subsequently, the catalyst was prepared by wet impregnation of the support, following the methodology described below: the support and precursor salt solutions, palladium chloride ($PdCl_2$) and indium chloride ($InCl_3$), were placed in a beaker to obtain the desired metal loadings: 1 wt% Pd and 0.25 wt% In. This metal ratio was chosen based on previous experiments where it was found that the catalytic activity decreased when modifying this mass ratio (4:1) [4]. Next, the suspension was heated to 80°C with magnetic stirring until total evaporation of the liquid and was kept in a furnace at 80°C for 12 h. Subsequently, the catalyst was calcined in a muffle furnace for 4 h at 500°C. Then, the precursor of the active phase was reduced by a 0.2 M hydrazine solution at 40°C for 1 h. After this time, the dark gray solid was filtered and washed five times with deionized water to remove the residual hydrazine, and finally the catalyst was dried in an oven at 80°C for 12 h. Hydrazine is a crucial element in catalyst preparation, serving as a reducing agent that profoundly impacts the formation and properties, including morphology and composition, of the catalyst. This influence extends to the catalytic activity and selectivity of the catalyst [22,23].

Catalyst characterization

The synthesized material was characterized before and after the reaction. The XRD patterns of the catalysts were acquired using an XD-D1 Shimadzu instrument with CuKα radiation operating at 30 kV and 40 mA. The scan rate employed was 2°/min within the $2\theta = 10^\circ$–90° range. XPS conduced with a technique system with a dual Mg/Al X-ray source and a hemispherical PHOI-BOS 150 analyzer in the fixed analyzer transmission mode. Spectra were acquired with a 30 eV-200 W and MgKX source and CasaXPS software processed the data to estimate relative elemental proportions after sample dehydration and exposure to ultra-high vacuum. SEM images were obtained using a Phenom World PRO X scanning electron microscope equipped with an energy-dispersive X-ray analysis system (EDX). Using ImageJ (free software, version 1.45), particle size and distribution were determined.

Initial nitrate reduction tests

The preliminary experiments involved utilizing a γ-Al_2O_3 support with known initial nitrate concentrations (100 N ppm, 50 N ppm, and 25 N ppm) to evaluate catalytic activity for nitrate reduction. These tests were conducted in the presence of stoichiometric amounts of the reducing agent, formic acid (HCOOH), with a ratio of 5:2 HCOOH to NO_3^-. The monometallic Pd catalyst (1 wt%/γ-Al_2O_3) and monometallic In catalyst (0.25 wt%/ γ-Al_2O_3) were also subjected to nitrate reduction assessments under similar conditions.

Catalytic nitrate reduction

Nitrate elimination reactions were performed in a 250 mL batch reactor with 3 inlets, operated with magnetic stirring (at 800 RPM) and temperature control (maintained at 25°C). The initial concentration of nitrate in the reaction medium was 25, 50, or 100 ppm N-NO_3, with 200 mg of catalyst and formic acid as the reducing agent, and a final total reaction volume of 80 mL. The concentrations used in each reaction are shown in Table 1, where the "FA" in the label means the stoichiometric concentration for nitrate elimination using formic acid as the reducing agent (Eq. 1) [10], and the "N" nomenclature represents the concentration of N-NO_3^- in ppm, and the numbers “4, 5 and 6” represents the pH of the reaction. For pH correction, a 0.1 M. FA solution was used in insignificant quantities compared to the concentration of the reagents.

High nitrate concentrations can be found in the tertiary treatment of water and wastewater treatment plants, such as electrodialysis, producing a concentrated stream. Concentrations of nitrate from electrodialysis are between 300 and 1600 mg/L [22,23].

$$2NO_3^-(aq) + 5HCOOH(aq) \xrightarrow{Pd-In/Al2O3} N_2(g) + 3CO_2(g) + 2HCO_3^-(aq) + H_2O(l) \qquad (1)$$

The pH control with formic acid has been studied in a previous work [24], and it was found that control with formic acid promotes a lower selectivity towards NH_4^+ up to ten times lower than that obtained compared to H_2 as the reducing agent.

The UV-Vis spectrophotometer (Cole Parmer 1100) was employed to analyze the concentrations of NO_3^-, NO_2^-, and NH_4^+ ions using the Griess method [25] for nitrites and nitrates (absorbance at 543 nm) and the modified Berthelot method [26] for ammonium (absorbance at 633 nm). The conversions are expressed in % and represent the amount of nitrate removed during the evaluation time. The selectivities for the different nitrogen species are expressed in % and are calculated according to Eq. 2.

Table 1
Tests with different concentrations of FA and, using Pd1(wt%) In0.25(wt%)/Alumina catalyst.

Test	$C^0_{NO_3^-}$ (N-ppm)	C^0_{FA} (x10^{-3} M)	pH	pH adjustment solution*
N100–0.5FA-5	100	8.9	5.0	FA
N100-FA-5	100	17.8	5.0	FA
N100–2FA-5	100	35.6	5.0	FA
N100–3FA-5	100	53.4	5.0	FA
N50-FA-5	50	8.9	5.0	FA
N50–2FA-5	50	17.8	5.0	FA
N25-FA-5	25	4.5	5.0	FA
N25–2FA-5	25	8.9	5.0	FA
N100-FA-5-HCl	100	17.8	5.0	HCl
N100-FA-5-WC	100	17.8	5.0	Without control**
N100-FA-4	100	17.8	4.0	FA
N100-FA-6	100	17.8	6.0	FA

$C^0_{NO_3^-}$ Initial concentration of nitrate

C^0_{FA} (10^{-3} M) Initial concentration of formic acid (FA).

*pH adjustment solutions: FA 0.4 M; HCl 0.1 M. **The pH was adjusted to 5.0 (or 4 or 6 when corresponds) at the beginning of the reaction and then was not further corrected.

$$S(\%) = [C_A/(C_0 - C)] \times 100 \qquad (2)$$

Where C is the N-ppm of nitrates at time t, C_0 is the N-ppm of nitrates at the beginning of the reduction process, and C_A is the N-ppm of products (nitrite or ammonium) at time t. The nitrogen selectivity was calculated by subtracting the selectivities obtained for nitrite and ammonium, considering that the formation of nitrogen oxides is insignificant.

The initial reaction rate (v_i) is calculated by considering the time required to convert 10% of the initial nitrate concentration, given in ppm/min. The method employed for calculating initial reaction rates (vi) aligns with established practices in the literature, as evidenced by studies [10,27,28]. Sacco et al. [27] specifically note that the initial rate (vi, given in ppm/min) is estimated considering that, up to 10% conversion, the system remains unaffected by its reaction products. This methodology ensures that the initial rate is determined under conditions where the system is minimally impacted by reaction products, providing a robust measure of the intrinsic catalytic activity. The initial rates method is based on the assumption that the concentration of each reactant and the temperature remain relatively constant throughout the time interval during which the reaction rate is being assessed [29,30].

Results and discussion

Initial nitrate reduction tests

The objective of this phase was to investigate the catalytic capability of both the individual support (γ-Al_2O_3) and catalysts (Pd 1 wt%/γ-Al_2O_3 and In 0.25 wt%/γ-Al_2O_3) when exposed to stoichiometric amounts of the reducing agent, formic acid. After a 2-hour examination period, as illustrated in Figures S1, S2, and S3 (available in the Supplementary Material), it was confirmed that nitrates did not undergo catalytic reduction. These findings provide valuable insights into the behavior of monometallic Pd and In catalysts, shedding light on their performance under these specific conditions.

Recent studies, such as the one conducted by Sacco et al. [27], have demonstrated that Pd/In catalysts supported on alumina exhibit high performance in nitrate removal from water. Sacco et al. reported that the nitrate removal order was $Al_2O_3 > TiO_2 > SiO_2$, with alumina-based catalysts showing the highest selectivity towards N_2 due to a strong metal-support interaction. This strong metal-support interaction enhances the dispersion of Pd and In on the alumina surface, likely leading to an increase in the number of active catalytic sites and, consequently, improved reaction activity and selectivity. Furthermore, alumina is a widely used support in catalytic processes due to its high surface area, thermal stability, and cost-effectiveness. Its ease of functionalization allows fine-tuning of surface properties to further optimize catalyst performance.

Effect of initial concentration of formic acid on catalytic reduction

Fig. 1a illustrates the nitrate conversion over time for varying initial concentrations of the reducing agent. When the formic acid concentration was triple the stoichiometric ratio with respect to nitrate, complete nitrate conversion wasn’t achieved within 120 minutes. Conversely, with sub-stoichiometric amounts, nitrate reduction was constrained by the reducing agent concentration (limiting reactant).

Fig. 1b shows that the reaction operating with formic acid limitation (N100–0.5FA-5) generates less nitrite. This behavior is acceptable, as it

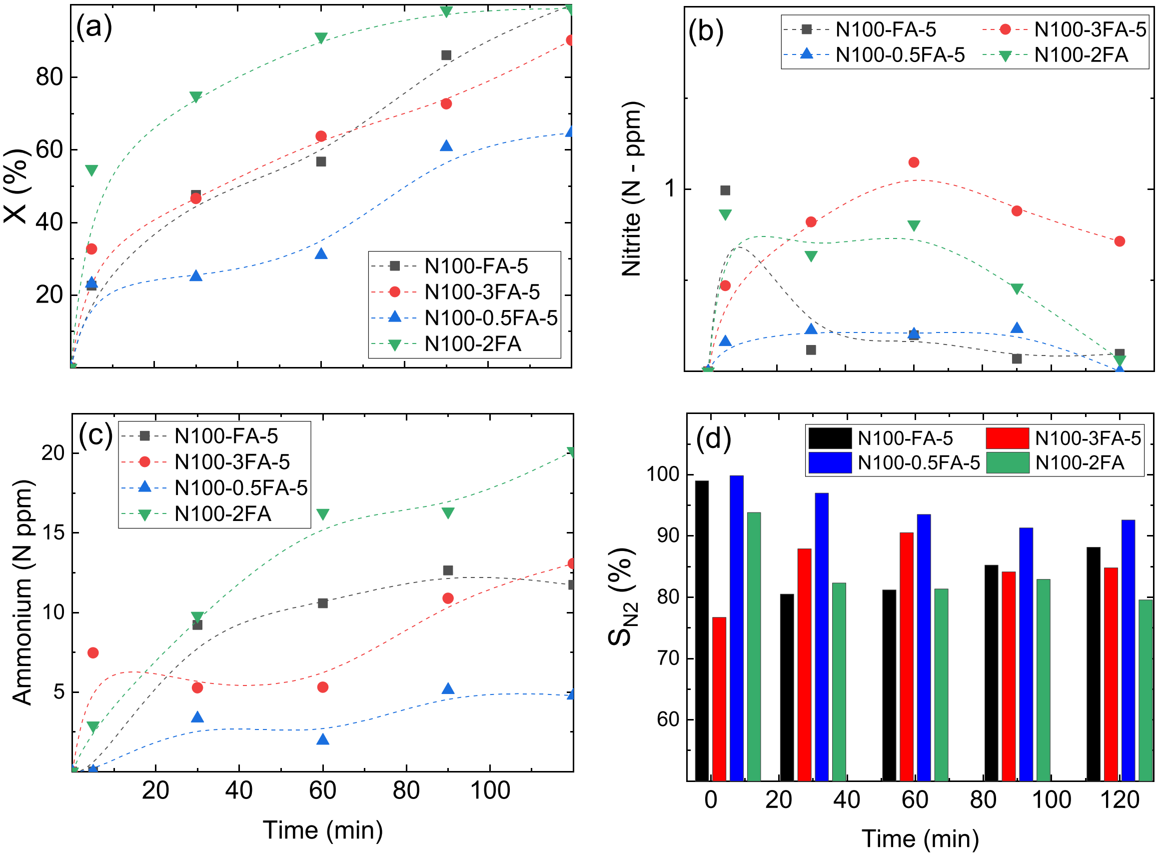

Fig. 1. (a) Nitrate conversion versus time at different concentrations of reducing agent. Concentrations of (b) nitrite, (c) ammonium, versus time using different initial concentrations of formic acid. (d) Nitrogen selectivity at different reaction times. Conditions: Initial nitrate concentration: 100 N ppm, pH 5, pH correction with 0.1 M FA.

was observed above that the initial reaction rate is half of the initial rate when using the stoichiometric ratio. N100-FA-5 and N100–2FA-5 have very similar rates of nitrite formation in the first 5 minutes; however, N100–2FA-5 has a slower consumption of nitrite, which could indicate that having twice as many species of reducing agents in the catalytic system may be saturating the surface of the catalyst and inhibiting the successive nitrite reduction reaction. Alternatively, the presence of ubiquitous negative ions on the catalyst's surface could be repelled by electrostatic forces, preventing the nitrites from approaching the active surface. Moreover, the high concentration of species in the reaction medium could even be obstructing the arrival of nitrites to the catalyst's surface.

It can be seen in Fig. 1c that the lower formation of ammonium corresponds to the lowest catalytic activity among the evaluated reactions (N100–0.5FA-5). It can also be observed that in N100–2FA-5, more ammonium formation was obtained. On the other hand, N100–3FA-5 converted a proportion lower than twice that, so it can be suggested that surface saturation prevents over-hydrogenation, decreasing the selectivity for NH_4^+ formation.

Fig. 1d displays the nitrogen selectivity values, showing fluctuations corresponding to the generation of reaction products, namely ammonium and nitrite. Nitrite, acting as a reaction intermediate, nearly disappears entirely within 120 minutes.

Among the four concentration levels assessed in this stage, N100–0.5FA-5 demonstrates the highest SN_2, followed by N100-FA-5, when selectivity is compared at the same conversion level.

Comparing formic acid with hydrogen as the reducing agent [28], using a Pd,In/Alumina catalyst with the same metal loading, it was found that both completely convert nitrate. However, employing H_2 as the reducing agent, NO_3^- was completely converted in about 70 minutes, while with formic acid, complete conversion was achieved at 120 minutes. This is reasonable since in the first case, H_2 is provided in excess in the reaction medium, mainly due to its low solubility at this temperature. On the other hand, the formic acid molecule must adsorb on the surface of the catalyst and decompose to generate the adsorbed H [31–34] necessary to react with the nitrate ion. Hence, it is necessary for FA to first decompose on the Pd surface, and for H, which is now available for the reaction, to be in proximity to the nitrate and react with it to form nitrite [35].

Peláez et al.'s work [31] significantly contributes to the comprehension of catalytic reduction by underscoring the critical role of formic acid adsorption on the catalyst surface and its subsequent decomposition, aligning seamlessly with the ongoing discussion. As highlighted by Peláez et al., this process unfolds in multiple stages, potentially exerting a substantial influence on the overall reaction rate. In-depth investigations by Dong et al. [34] and Karatok et al. [33] delve into the intricate aspects of the catalyst's structure. Dong et al. focus on Pd-Au alloy structures [28], while Karatok et al. highlight Ag domains modified by subsurface-interacting Pd. These structural intricacies, as elucidated by Dong et al. and Karatok et al., underscore the multifaceted nature of formic acid decomposition. This underscores the idea of multiple sequential stages influencing the overall reaction rate, complementing the concepts discussed in this section. The emphasis by Bhandari et al. [36] on self-consistent microkinetic models in terms of coverage and the role of spectator species like CO resonates with the importance of considering the complex interplay of factors during FA decomposition. Integrating these insights along with the nuanced details provided by Osipova et al. [32], who demonstrated the catalytic decomposition of formic acid into H_2/CO_2 under mild conditions, enhances our overall understanding of the intricate mechanisms governing formic acid decomposition and its relevance in catalytic processes.

Furthermore, the surface properties of the catalyst also play a critical role in the catalytic activity. The catalyst used in the present work has a point of zero charge of 7.4 [10], the approach of negatively charged ions to the positively charged surface of the catalyst is facilitated. Therefore, working at an acidic pH represents an advantage over neutral and basic pH for the evaluated conditions In this context, various forms of molecule aggregation in water [37,38], the greater polarization of formic acid, stemming from the negative charges in its molecular structure, promotes a closer interaction with the catalyst surface, in contrast to molecular hydrogen, which has been extensively used in the past for nitrate reduction [39–41] In fact, Jeon and Chung [42] investigated Pd/C catalysts for formic acid dehydrogenation, finding a volcano-type relationship between activity and pH. They observed enhanced catalytic activity for nitrate reduction at lower pH levels. The critical effect of the support on performance is attributed to factors like formate ion recombination and competitive adsorption [43] in acidic or basic solutions.

Following the discussion on the catalytic reduction of nitrate using formic acid, it is noteworthy to consider the possibility of removing residual formic acid from the process. A potential approach involves employing UV-based and electrochemical processes for formic acid mineralization from the effluent generated during the catalytic reduction reaction [19]. The results of the study indicate that direct photolysis alone is not sufficient for formic acid mineralization. However, heterogeneous photocatalysis, photo-assisted electrochemical oxidation, and electrochemical oxidation are effective methods for achieving formic acid mineralization. Among these, electrochemical oxidation demonstrated superior results with minimal energy consumption. This suggests a viable strategy for addressing the issue of non-reacted formic acid, contributing to the overall efficiency and environmental sustainability of the catalytic nitrate reduction process.

Table 2 shows the initial velocities of each reaction and selectivities for N_2 at the same conversion and the final products of nitrate reduction.

Table 2 presents a comprehensive analysis of the selectivities for N_2 and the final products of nitrate reduction under different experimental conditions. It can be observed that the initial reaction rate is directly proportional to the initial concentration of formic acid. The initial rate is halved when the initial concentration of FA is reduced by half, and the initial rate is tripled when the initial concentration of FA is doubled. These findings suggest a direct relationship between catalytic activity and the initial concentration of formic acid. It has been demonstrated in a previous study [10] that the presence of nitrate favors the decomposition of formic acid on the surface of Pd. However, when the FA concentration increases, other surface interactions start to act, such as steric hindrance of active sites, which has been reported in a study [10].

This would justify the catalytic behavior found in N100–3FA-5 since even though the initial velocity tripled, it did not favor catalytic activity to the same extent. It was observed that at the end of the control time, the reaction did not achieve 100% elimination of the contaminant. Therefore, a higher amount of reducing agent promotes a higher initial reaction rate, but up to an optimal point, and then it would act with the opposite effect, due to steric hindrance that excess ions in the medium would provide on the catalyst surface, which is what happens when the amount of FA is increased threefold. In general, the initial rates were high, with the velocity of N100–2FA-5 being comparable to that found with the same reaction and catalyst, using H_2 as a reducing agent in excess ($v_i = 11.2$ ppm/min, [4]). In the case of H_2 on the Pd surface, it undergoes a dissociative adsorption process, promptly rendering H available for participation in the reduction reaction [44]. However, in the case of FA, the initial step involves adsorption, followed by subsequent decomposition. At this point, dissociated H is ready to participate in the reduction reaction of nitrate or nitrite. The speed difference between decomposition and adsorption and dissociative adsorption can vary based on several factors, including specific reaction conditions, the types of molecules involved, and the catalyst's surface properties [45]. Generally, dissociative adsorption tends to occur more rapidly than decomposition and adsorption. This process involves a molecule being adsorbed onto the catalyst's surface and subsequently breaking down into smaller fragments. These smaller fragments can interact more efficiently with other reactants, thereby accelerating the overall reaction rate due to increased availability of active sites on the catalyst's surface.

In contrast, in decomposition and adsorption, the molecule is initially adsorbed in its intact form and then undergoes decomposition on the catalyst's surface. This process can be comparatively slower because the entire molecule must be adsorbed before the decomposition reaction can take place. Considering that the FA molecule is significantly larger than H_2 and likely possesses a larger coordination sphere, the potential for interaction with the catalyst's surface becomes more challenging and constrained, both in terms of space and electrical properties. This is because both molecules function as dipoles with distinct polarizations. It is essential to emphasize that the relative speed of these processes may fluctuate depending on the specific conditions and the characteristics of the reactants and active sites involved in the nitrate or nitrite reduction reaction [46–48].

Regarding selectivities, the observed behavior is that as the limitation of reducing agent on the catalyst surface increases, it favors N_2 selectivity. This occurs in the N100-FA/2 reaction, where an optimal compromise is reached between activity and N_2 selectivity at stoichiometric concentration, and then in N100–2FA-5, activity increases at the expense of N_2 selectivity. Finally, in N100–3FA-5, a decrease in catalytic activity and an increase in N_2 selectivity are observed. The best compromise ratio observed is in the stoichiometric reaction, N100-FA-5, with 88.2% selectivity to N_2.

In addition to the observed trends in selectivities, it is crucial to consider the potential impact of deactivation and CO poisoning on the catalytic performance, as elucidated by our group [49]. The study conducted stability tests by repeating nitrate reduction reactions under various conditions, including the use of oxoanions to assess competitive adsorption with nitrate and formic acid as the reducing agent. Notably, the catalyst used in these experiments is a Pd1%In0.25%/Alumina catalyst, prepared in pellet form. Interestingly, the catalyst exhibited a partial deactivation, and the material's activity was successfully recovered after washing with water. In the Fourier Transform Infrared (FTIR) spectroscopy analysis, no signals corresponding to CO were detected. This observation raises the possibility that the observed deactivation may not be solely attributed to CO poisoning. This aligns with the reversible nature of the deactivation, highlighting that competitive adsorption of anions on the catalyst is temporary. It is important to note that while FTIR is effective in detecting CO in chemisorption tests when

Table 2
Initial velocities and selectivity towards N_2 at the same conversion and final products of nitrate reduction.

	v_i (ppm/min)	v_i/v_i^{FA}	$\%S_{N_2}$	$\%S_{N_2}^{120'}$	$\%X^{120'}$	$[NH_4]^{120'}$ (N-ppm)	$[NO_2]^{120'}$
N100–0.5FA-5	2.1	0.5	92.3	92.1	60.0	4.8	n. d.
N100-FA-5	4.4	1.0	83.4	88.2	100	11.7	0.1
N100–2FA-5	15.4	3.0	83.1	79.6	99.0	20.0	0.1
N100–3FA-5	6.5	1.6	90.6	84.8	90.0	13.0	0.7

n.d. no detectable

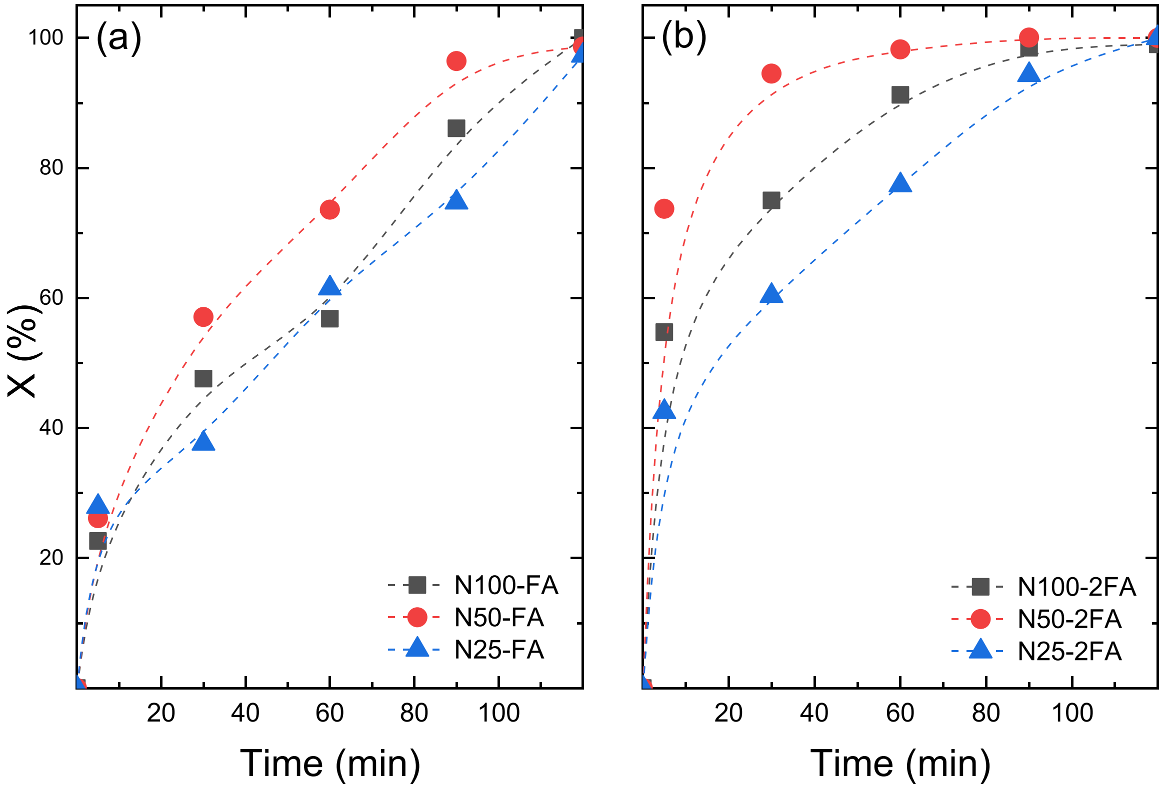

Fig. 2. (a) Nitrate conversion versus time at different initial nitrate concentrations employing a stoichiometric ratio of formic acid to nitrate. (b) Nitrate conversion versus time at different initial nitrate concentrations, utilizing twice the stoichiometric ratio of reducing agent to nitrate. Conditions: Initial nitrate concentration: 100 N ppm, pH 5, pH correction with 0.4 M formic acid.

the active phase is saturated with CO, its sensitivity may be limited in identifying CO in the reaction medium, where concentrations are lower.

Effect of the initial concentration of nitrate on catalytic reduction

In Fig. 2, conversions of nitrate are graphed against reaction time at pH 5.0. The initial nitrate concentrations were varied (100, 50, and 25 N-ppm), while employing both stoichiometric and double the stoichiometric initial concentrations of formic acid relative to nitrate concentration. This variation in formic acid concentrations provides a comprehensive view of the reaction kinetics and its dependency on the reductant-to-contaminant ratio.

It can be observed that a total conversion of nitrates is obtained at the three evaluated initial concentrations. What varies is the initial reaction rate.

The Table 3 presents the results of the initial reaction rates (v_i) and their ratios ($v_i/v_{i(FA)}$) for different reaction conditions involving varying nitrate concentrations and formic acid concentrations. The $v_i/v_{i(FA)}$ values represent the initial reaction rate observed in relation to the equivalent stoichiometric concentration reaction.

Comparing initial rates (v_i), a clear correlation emerges: a halving of NO_3^- concentration (100 N ppm to 50 N ppm to 25 N ppm) results in approximately a 50% reduction in the reaction rate, showcasing the direct relationship between initial concentration and rate with this catalyst. Examining specific scenarios, N100–2FA-5 exhibits a significantly higher initial rate (15.38 ppm/min), with a $v_i/v_i(FA)$ value of 3.52, indicating a 3.5-fold acceleration compared to the stoichiometric N100-FA-5 reference. This acceleration aligns with Choi et al.'s observation [50] that formic acid decay, without nitrate, is slightly slower than with nitrate, implying pollutant-induced acceleration in formic acid decomposition. Similarly, N50–2FA-5 and N25–2FA-5 both display notable increases in initial rates at 8.77 ppm/min and 2.45 ppm/min, respectively. Their $v_i/v_{i(FA)}$ values of 3.51 and 1.88 affirm that doubling the formic acid concentration significantly accelerates the reaction rate, even at lower nitrate concentrations. In summary, doubling the stoichiometric formic acid concentration remarkably enhances initial reaction rates across all nitrate concentrations. This underscores the promoting effect of excess reducing agent (formic acid) on reaction kinetics, leading to higher conversion rates. The $v_i/v_{i(FA)}$ ratios vividly illustrate that employing double the stoichiometric formic acid concentration yields notably higher reaction rates compared to their stoichiometric counterparts.

In Fig. 3, we can observe the nitrogen selectivities achieved during nitrate conversion using different initial nitrate concentrations, and evaluating the best results obtained from the previous run, i.e., stoichiometric concentration and twice the stoichiometric concentration.

It can be observed in Fig. 3 that selectivities are higher at the initial concentrations of nitrate NO_3^- of 25 N ppm, both when using the stoichiometric concentration (FA-5) and the double stoichiometric concentration (2FA-5) of reducing agent, compared to nitrate. The observed trend was that at 25 ppm of N, higher N_2 selectivity was achieved compared to 50 ppm of N, and even higher selectivity compared to 100 ppm of N. This phenomenon could potentially be linked to the hypothesis that active sites have lower levels of saturation by contaminants. Alternatively, it might stem from the presence of a greater

Table 3
Initial Reaction Rates and v_i/v_i^{FA} ratios for different reaction conditions.

	v_i	v_i/v_i^{FA}
N100-FA-5	4.36	1.00
N50-FA-5	2.50	1.00
N25-FA-5	1.30	1.00
N100–2FA-5	15.38	3.52
N50–2FA-5	8.77	3.51
N25–2FA-5	2.45	1.88

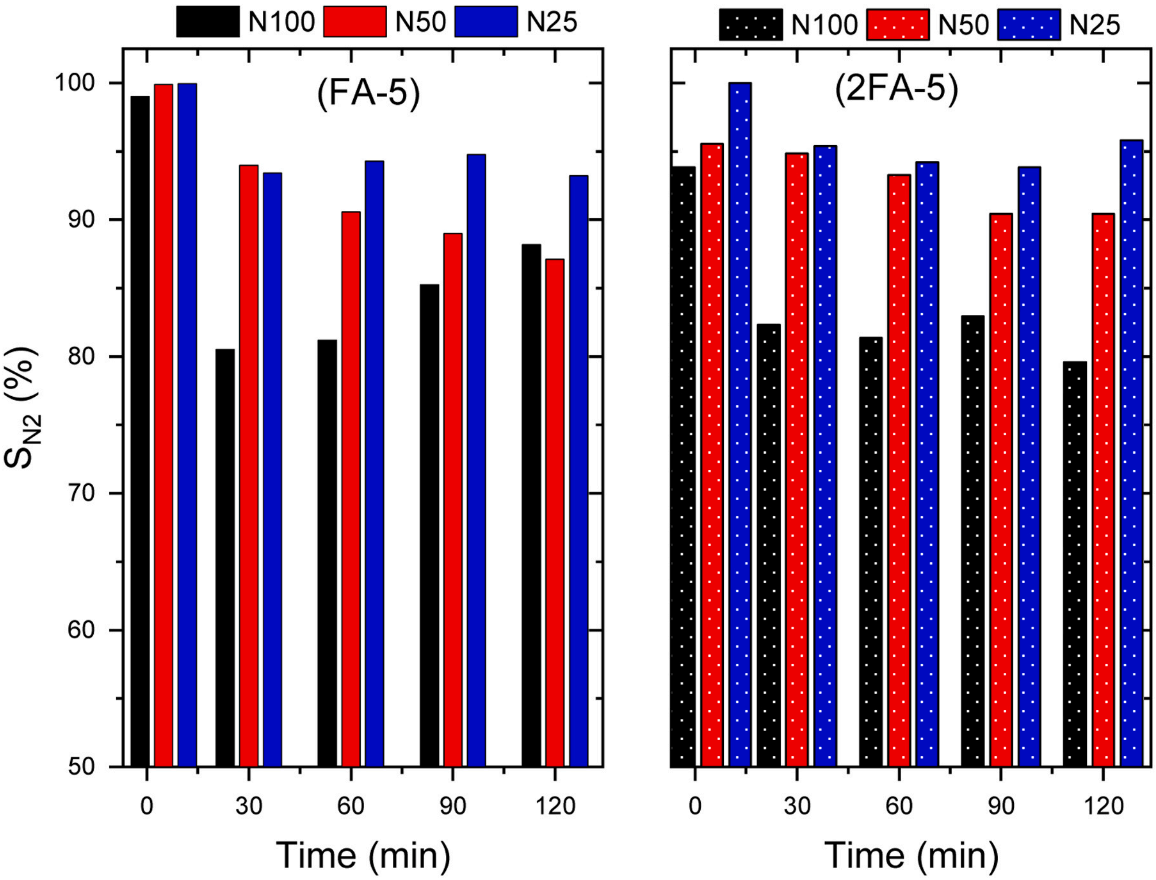

Fig. 3. Gas-phase nitrogen selectivity for reactions with different initial concentrations of nitrate and formic acid.

number of available sites when initiating the reaction with 25 N ppm, in contrast to commencing with N 100 ppm, for instance.

Effect of pH on nitrate reduction

Fig. 4 shows the dependence of nitrate conversion (Fig. 4a) and selectivity to the gas phase N_2 (Fig. 4b) on the reaction pH. In one of the cases, the reaction pH was maintained by adding FA at 4.0, 5.0, and 6.0 (N100-FA-pH), or HCl at pH = 5.0 (N100-FA-5-HCl). In another case, the pH was worked without pH control (N100-FA-5-WC). For an initial pH of 5.0, in the N100-FA-5-WC assay, the catalytic activity decreased markedly with reaction time, while for the assay where the pH was controlled with HCl, the nitrate conversion stagnated after 30 minutes of reaction, probably due to FA depletion. On the other hand, when FA was used for pH control, full nitrate conversion was achieved. This difference can be attributed to formic acid's dual role: not only regulates the pH, but it also acts as a replenishing source for the reducing agent within the medium. This observation aligns with previous reports [39] indicating that without pH control, the nitrate reduction reaction tends to cease earlier, leaving nitrites as the main product.

In Fig. 4-a, the conversion versus time is depicted, showcasing the impact of pH control on catalytic nitrate reduction under the previously described distinct conditions. These conditions include: maintaining control using formic acid (FA) at pH 4.0, 5.0, and 6.0; employing hydrochloric acid (HCl) for control; and observing the scenario without the addition of any pH regulator (WC). Given that formic acid dissociates into hydrogen ions (H^+) and formate ions ($HCOO^-$) in water, the presence of this dissociation is also pertinent to the bimetallic palladium-indium catalyst. At lower pH levels, a higher concentration of hydrogen ions (H^+) prevails. This elevated concentration may impact the dissociation of formic acid and heighten the accessibility of reducing species [51]. Consequently, this phenomenon has the potential to amplify the effectiveness of formic acid as a reductive agent in the process of nitrate reduction. This influence of pH on the catalytic activity sets the stage for the exploration of a characteristic behavior known as the volcano-type curve.

In terms of selectivity towards N_2, elevated values were achieved through the reaction FA-5-HCl, despite this reaction exhibiting a nitrate conversion of only 40%.

The pH range of 4.0–5.0 significantly enhances nitrate reduction, with optimal performance observed. Notably, at pH 6, catalytic activity decreases. This behavior aligns with literature on formic acid dehydrogenation, where a volcanic curve links activity to pH [42]. The current study emphasizes the correlation between acidic pH and heightened catalytic activity in nitrate reduction. It explores the influence of the support material, highlighting factors like formate ion recombination and competitive adsorption with hydroxide ions. The catalyst's surface properties, with an isoelectric point of 7.4, contribute to this behavior. At pH 5, formic acid predominantly exists as dissociated formate ions, positively charged alumina surface electrostatically attracting negatively charged species. This condition enhances catalytic activity by facilitating the presence of dissociated formate ions on the catalyst's surface. Importantly, the study doesn't address formic acid decomposition. In a previous study with similar material (Pd1(wt%) In0.25(wt%) /Alumina) [10], it was observed that the catalytic activity, concerning pH, follows a volcano-shaped curve, assessing pH from 3.0 to 7.5. Catalytic activity at pH 3 is lower than at pH 4.0 and 5.0, and from pH 6.0 to pH 7.5, there is also a decline in catalytic activity. For this material, the optimal pH range for enhanced catalytic activity lies between pH 4 and 5. Overall, understanding these pH-related influences provides insights into optimizing catalytic performance in nitrate reduction.

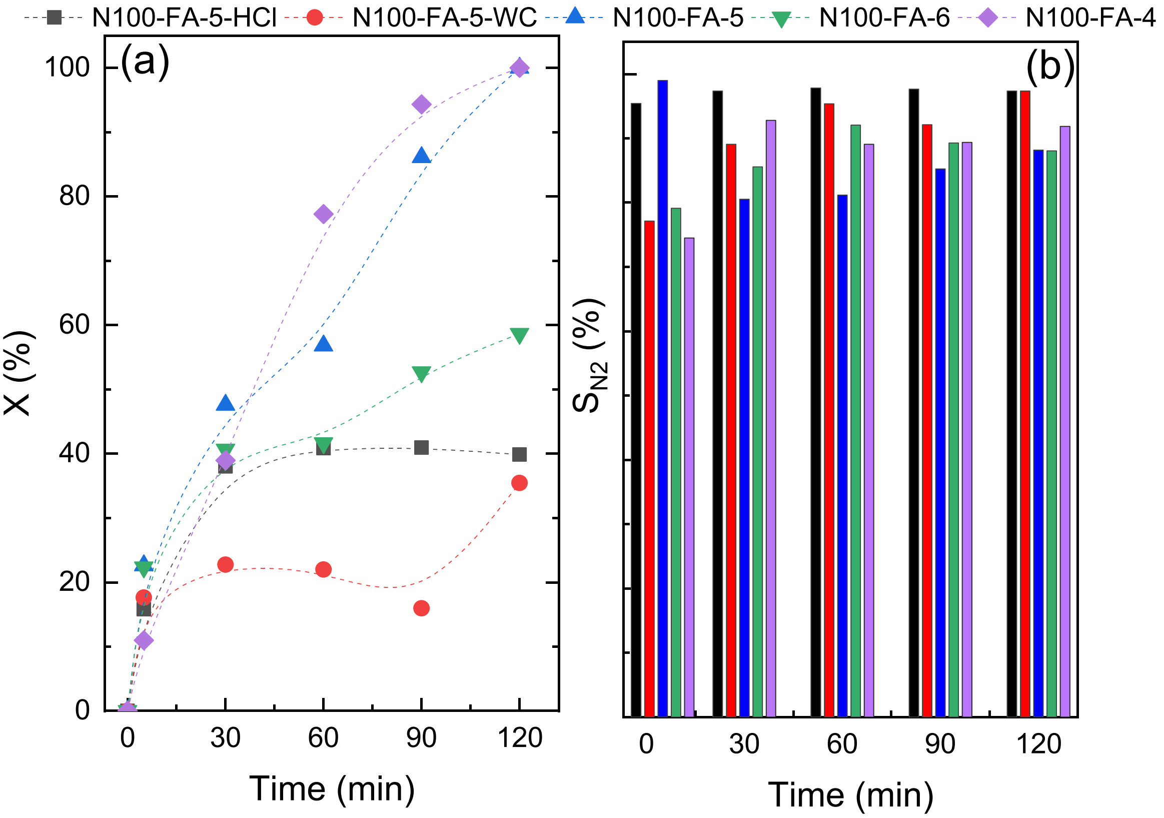

Fig. 4. (a) Conversion vs. Time at Various pH and Control Settings. (b) Gas-Phase Nitrogen Selectivity under the Same Conditions. Initial nitrate concentration: 100 ppm N; Initial reducing agent concentration: $1.78 \cdot 10^{-2}$ M.

Catalyst characterization

The catalyst used in the present work has already been extensively characterized in a previous study [10]. In summary, the dispersions of the fresh and used catalyst are 35% and 39%, respectively (data obtained by dynamic H_2 chemisorption). The dispersion increased by approximately 11% after contact with the reaction medium. With the X-ray Photoelectron Spectroscopy (XPS) technique, both Pd° and Pd^{2+} components were observed in the fresh catalyst (after being reduced with H_2 and N_2H_4). BE which is directly associated with the higher oxidation states of the Pd (BE Pd^0 334.9 eV, PdO 336.0 eV) [52]. The highest binding energy corresponds to Pd^{2+} (associated with oxidized palladium forms), and the lowest binding energy is associated with metallic Pd. It is noteworthy that in the sample reduced with hydrazine, where the main component was metallic Pd (84%), whereas in the H_2-reduced one, this component accounted for only 55% of the total Pd $3d_{5/2}$. This difference in surface composition could explain better activity in reducing nitrites and decomposing HCOOH. Indium showed

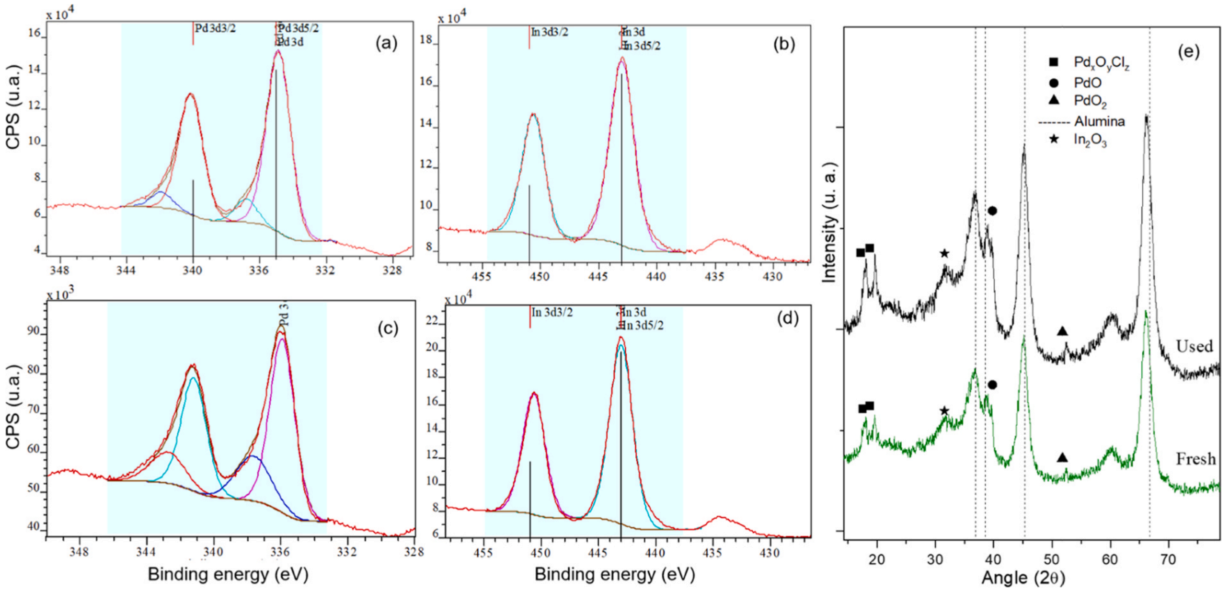

Fig. 5. (a) and (c) Pd XPS Spectra, (b) and (d) In XPS Spectra of Pd,In/Al_2O_3 1:0,25 wt%; (e) DRX Patterns of fresh and used Pd,In/Al_2O_3 1:0,25 wt% catalyst.

only one component associated with metallic In°. The catalysts exhibited an increase in the Pd/Al ratio after the reaction, suggesting that the surface was enriched with Pd. In Fig. 5, panels (a) and (c) depict the XPS spectra of Pd, while in Fig. 5, panels (b) and (d) present the In XPS spectra acquired for the Pd1(wt%) In0.25(wt%)/Al_2O_3 catalyst samples before reduction with N_2H_4 (a, b) and with H_2 (c, d). Additionally, Fig. 5 (e) displays the diffractograms of the catalysts employed in this study.

Fig. 5(e) presents the X-ray diffraction (XRD) patterns Pd1(wt%) In0.25(wt%)/Alumina-supported catalysts. The patterns of catalysts prepared before the reaction (Fresh catalyst) and after the reaction (used catalyst, N100-FA) reveal distinct peaks corresponding to Al_2O_3, observed at 36.7°, 40.0°, 45.7°, and 66.7°. However, no signals corresponding to In_2O_3 or Pd^0 are detected in the fresh sample. This suggests that the metal or oxide particles on Al_2O_3 are highly dispersed or possibly fall below the detection limit of the XRD system due to the low catalyst load. The faint signals at lower angles in the fresh and used samples are attributed to Pd_2OCl_2 species, likely originating from the precursor salts. While the faint signals at lower angles in both fresh and used samples can be attributed to Pd_2OCl_2 species, their presence is noteworthy. Despite employing hydrazine reduction, some residual surface oxidation might remain due to various factors, such as insufficient reaction time, temperature, or potentially hindered access of hydrazine to all catalyst sites. The slight increase in these Pd_2OCl_2 peak intensities in the used catalyst further supports this hypothesis, suggesting possible reoxidation under reaction conditions. The presence of both oxidized and reduced forms can be associated with the redox process involved during catalyst preparation and use. Notably, at around 52°, the signal of indium oxide (PDF 6–416) is detected, and its intensity increases in the used sample, consistent with the redox process. Additionally, at 39.2°, a distortion appears in the characteristic peak of alumina, which may result from the contribution of the diffraction of In (110) (PDF 5–642) or possibly associated with the diffraction peak of metallic Pd at 39.7°. These results are in line with those obtained in a previous study by the group [10].

Fig. 6 includes SEM micrographs providing valuable insights into the catalyst synthesized for this study, Pd1(wt%) In0.25(wt%)/Alumina

Concerning the fresh catalyst (Fig. 6-a), we observe a presence of agglomerates alongside what appears to be a uniform particle distribution on the surface. It's important to note that SEM, while useful for identifying agglomerates, may not provide the resolution required to precisely determine nanoparticle size within the range defining good dispersion. The EDS analysis indicates that these agglomerates contain palladium and indium in a mass ratio of four, with a medium size of 5 nm (40%). Additionally, another significant population of particles or agglomerates (not shown) ranging in size from 300 to 900 nm is identified, constituting 35% of the total, following previous study [10]. In the used sample (Fig. 6-b), the particles vary in size reaching a medium size of 9 nm, comprising approximately 30% of the particles, while 50% of the population forms aggregates with sizes between 100 and 800 nm. The smaller particles tend to aggregate, leading to an increase in the percentage of larger particles. This behavior was previously observed in a previous study [10]. In used sample Pd is detectable on the larger particles, exhibiting various prismatic shapes, with bimetallic particles also present on the surface. The Pd:In ratio remains constant, approximately five, and the particle distribution remains homogeneous. This unexpected result of good surface particle distribution aligns with observations made through the H_2 chemisorption technique. Notably, catalysts with low metal loading demonstrate performance equal to or higher than those reported in the literature for the same reaction, highlighting the economic advantages associated with producing catalysts with low metallic loading.

Conclusions

A (Pd, In)-based catalyst with a Pd loading of 1 wt% and In loading of 0.25 wt%, synthesized onto alumina, was prepared and assessed for its efficacy in removing nitrate from water. The study aimed to explore the impact of various parameters on the catalytic performance and selectivity, resulting in the achievement of high efficiency in the catalytic reduction of nitrate.

The study emphasizes the importance of selecting appropriate conditions, such as initial concentrations of formic acid and nitrate, as well as pH control, on catalytic performance. to balance catalytic activity and N_2 selectivity.

The reaction rate increases with higher formic acid concentrations up to an optimal point, after which excess formic acid inhibits the reaction due to surface saturation. The best compromise between activity and N_2 selectivity is achieved at stoichiometric formic acid concentration. Higher initial nitrate concentrations lead to faster initial reaction rates. Doubling the stoichiometric formic acid concentration accelerates

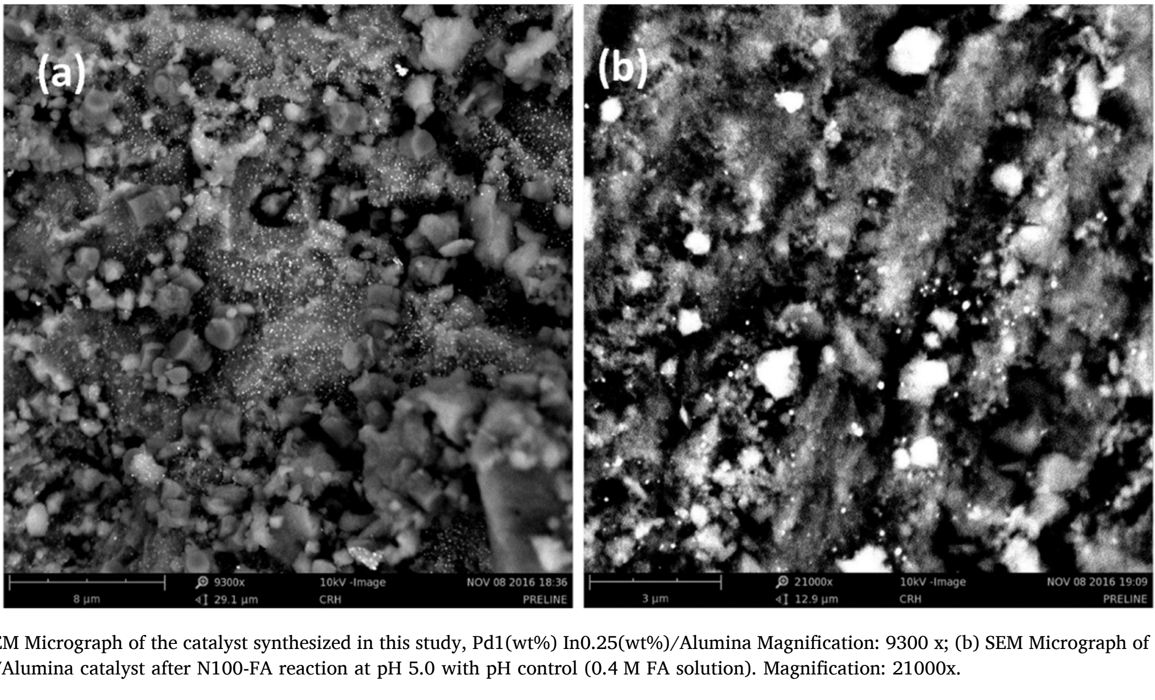

Fig. 6. (a) SEM Micrograph of the catalyst synthesized in this study, Pd1(wt%) In0.25(wt%)/Alumina Magnification: 9300 x; (b) SEM Micrograph of the Pd1(wt%) In0.25(wt%)/Alumina catalyst after N100-FA reaction at pH 5.0 with pH control (0.4 M FA solution). Magnification: 21000x.

reaction kinetics and conversion rates significantly. Controlling pH using formic acid as the regulator enhances catalytic activity and selectivity compared to using hydrochloric acid. The dissociation of formic acid into H^+ and $HCOO^-$ contributes to the effectiveness of formic acid as a reductive agent. A pH range of 4.0–5.0 enhances nitrate reduction, leading to comprehensive conversions and improved selectivity toward N_2.

Ethical Approval

Not applicable.

Funding

This work was supported by CONICET, MinCyT, FIQ-UNL, INCAPE, PICT 2019–02970, CAI+D 2020 50620190100148LI of Argentina and CYTED RECIRCULA 323RT0143.

Declaration of Competing Interest

The authors declare that they have no known competing financial interests or personal relationships that could have appeared to influence the work reported in this paper.

Acknowledgments

The authors wish to acknowledge the financial support of FIQ-UNL, INCAPE, PICT 2019–02970, CAI+D 2020 50620190100148LI of Argentina and CYTED RECIRCULA 323RT0143.

Authors contribution

F. M. Zoppas: Substantial contributions to the conception or design of the work; or the acquisition, analysis, or interpretation of data for the work. Final approval of the version to be published and agreement to be accountable for all aspects of the work in ensuring that questions related to the accuracy or integrity of any part of the work are appropriately investigated and resolved. *N. A. Sacco:* Conceptualization, formal analysis, investigation, writing original draft, writing-review and editing, and visualization. *T. Favarini Beltrame:* Rafting the work or revising it critically for important intellectual content. *F. Akhter:* Rafting the work or revising it critically for important intellectual content. *E. Miró:* Resourses, final approval of the version to be published. *F. A. Marchesini:* Resourses, writing-review and final approval of the version to be published

Consent to Participate

All the authors declare that they are consent to participate in this study.

Consent to Publish

All the authors declare that they are consent to publish this study.

Appendix A. Supporting information

Supplementary data associated with this article can be found in the online version at doi:10.1016/j.nxsust.2024.100030.

References

[1] G. Tokazhanov, E. Ramazanova, S. Hamid, S. Bae, W. Lee, Advances in the catalytic reduction of nitrate by metallic catalysts for high efficiency and N2 selectivity: a review, Chem. Eng. J. 384 (2020), https://doi.org/10.1016/j.cej.2019.123252.

[2] C. Wisniewski, F. Persin, T. Cherif, R. Sandeaux, A. Grasmick, C. Gavach, Denitrification of drinking water by the association of an electrodialysis process and a membrane bioreactor: feasibility and application, Desalination 139 (2001) 199–205, https://doi.org/10.1016/S0011-9164(01)00311-3.

[3] Y. Zhang, Y. Lv, Y. Mo, H. Li, P. Tang, D. Li, Y. Feng, Facile preparation and promising hydrothermal stability of spherical γ-alumina support with high specific surface area, Catalysts 12 (2022), https://doi.org/10.3390/catal12111416.

[4] F.A. Marchesini, S. Irusta, C. Querini, E. Miró, Spectroscopic and catalytic characterization of Pd-In and Pt-In supported on Al2O3 and SiO2, active catalysts for nitrate hydrogenation, Appl. Catal. A Gen. 348 (2008) 60–70, https://doi.org/10.1016/j.apcata.2008.06.026.

[5] J. Hirayama, Y. Kamiya, Tin-palladium supported on alumina as a highly active and selective catalyst for hydrogenation of nitrate in actual groundwater polluted with nitrate, Catal. Sci. Technol. 8 (2018), https://doi.org/10.1039/c8cy00730f.

[6] S.R. Mishra, V. Gadore, M. Ahmaruzzaman, Recent advances in In2S3-based photocatalysts for catalytic reduction of CO2, Chem. Phys. Impact 7 (2023) 100324, https://doi.org/10.1016/J.CHPHI.2023.100324.

[7] S.R. Mishra, V. Gadore, M. Ahmaruzzaman, Insights into persulfate-activated photodegradation of tinidazole and photoreduction of hexavalent chromium through β-In2S3 anchored on Ag-doped fish scale-derived HAp composite quantum dots, J. Clean. Prod. 427 (2023) 139221, https://doi.org/10.1016/J.JCLEPRO.2023.139221.

[8] S.R. Mishra, Md Ahmaruzzaman, Microplastics: identification, toxicity and their remediation from aqueous streams, Sep Purif. Rev. 52 (2023) 283–304, https://doi.org/10.1080/15422119.2022.2096071.

[9] F. Miranda Zoppas, N. Sacco, J. Soffietti, A. Devard, F. Akhter, F.A. Marchesini, Catalytic approaches for the removal of microplastics from water: Recent advances and future opportunities, Chem. Eng. J. Adv. 16 (2023) 100529, https://doi.org/10.1016/J.CEJA.2023.100529.

[10] F. M. Zoppas, A. M. Bernardes, E.E. Miró, F.A. Marchesini, Nitrate reduction of brines from water desalination plants employing a low metallic charge pd, in catalyst and formic acid as reducing agent, Catal. Lett. 148 (2018) 2572–2584, https://doi.org/10.1007/s10562-018-2429-x.

[11] W.G. Mook, Chemistry of carbonic acid in water, Environ. Isot. Hydrol. Cycle (2000) 271.

[12] F.A. Marchesini, N. Picard, E.E. Miró, Study of the interactions of Pd,In with SiO 2 and Al 2O 3 mixed supports as catalysts for the hydrogenation of nitrates in water, Catal. Commun. 21 (2012) 9–13, https://doi.org/10.1016/j.catcom.2012.01.015.

[13] R. Zhang, D. Shuai, K.A. Guy, J.R. Shapley, T.J. Strathmann, C.J. Werth, Elucidation of nitrate reduction mechanisms on a Pd-In bimetallic catalyst using isotope labeled nitrogen species, ChemCatChem 5 (2013) 313–321, https://doi.org/10.1002/cctc.201200457.

[14] U. Prüsse, K.D. Vorlop, Supported bimetallic palladium catalysts for water-phase nitrate reduction, J. Mol. Catal. A Chem. 173 (2001) 313–328, https://doi.org/10.1016/S1381-1169(01)00156-X.

[15] Y. Ding, W. Sun, W. Yang, Q. Li, Formic acid as the in-situ hydrogen source for catalytic reduction of nitrate in water by PdAg alloy nanoparticles supported on amine-functionalized SiO2, Appl. Catal. B 203 (2017) 372–380, https://doi.org/10.1016/j.apcatb.2016.10.048.

[16] N. Tong, Z. Xia, T. Xie, X. Liu, J. Shen, Z. Zhang, X. Wang, Photochemistry of nitrate ion: reduction by formic acid under UV irradiation, Photochem. Photobio. 98 (2022) 404–411, https://doi.org/10.1111/php.13518.

[17] F.M. Zoppas, T.F. Beltrame, F.A. Sosa, A.M. Bernardes, E. Miró, F.A. Marchesini, Superficial properties of activated carbon fiber catalysts produced by green synthesis and their application in water purification, Environ. Sci. Pollut. Res 27 (2020) 40405–40420, https://doi.org/10.1007/s11356-020-10012-x.

[18] F.M. Zoppas, A.M. Bernardes, E. Miró, F.A. Marchesini, Improving selectivity to dinitrogen using Palladium-Indium coated on activated carbon fibers: preparation, characterization and application in water-phase nitrate reduction using formic acid as an alternative reductant source, J. Environ. Chem. Eng. 6 (2018) 4764–4772, https://doi.org/10.1016/j.jece.2018.07.015.

[19] F.M. Zoppas, S.W. Da Silva, T.F. Beltrame, F.A. Marchesini, A.M. Bernardes, E. Miró, Mineralization of formic acid from catalytic nitrate reduction effluent by UV-based and electrochemical processes, J. Environ. Chem. Eng. 8 (2020) 104127, https://doi.org/10.1016/j.jece.2020.104127.

[20] Z. Yang, Z. Zhu, R. Luo, X. Qiu, J.T. Liu, J.K. Yang, W. Tang, Iridium-catalyzed highly efficient chemoselective reduction of aldehydes in water using formic acid as the hydrogen source, Green. Chem. 19 (2017) 3296–3301, https://doi.org/10.1039/c7gc01289f.

[21] H. Liu, X. Liu, Y. Yu, W. Yang, J. Li, M. Feng, H. Li, Bifunctional networked Ag/AgPd core/shell nanowires for the highly efficient dehydrogenation of formic acid and subsequent reduction of nitrate and nitrite in water, J. Mater. Chem. A Mater. 6 (2018) 4611–4616, https://doi.org/10.1039/c8ta00600h.

[22] Z. Jiao, M. Liu, Z. Wang, X. Ning, Y. Yang, S. Li, T. Liu, Ti3C2OH MXene supported NiPtP nanoparticles with low noble metal content as hydrazine dehydrogenation catalysts, J. Taiwan Inst. Chem. Eng. 146 (2023) 104794, https://doi.org/10.1016/J.JTICE.2023.104794.

[23] X. Wei, H. Dai, Y. Li, T. Wang, S. Li, Enhancement of catalytic properties and durability in Ni–B–P/Ni foam for hydrazine electrooxidation, Int J. Hydrog. Energy 48 (2023) 23866–23876, https://doi.org/10.1016/J.IJHYDENE.2023.03.225.

[24] A. Garron, K. Lázár, F. Epron, Effect of the support on tin distribution in Pd-Sn/Al2O 3 and Pd-Sn/SiO2 catalysts for application in water denitration, Appl. Catal. B 59 (2005) 57–69, https://doi.org/10.1016/j.apcatb.2005.01.002.

[25] W.C. Lipps, E.B. Braun-Howland, T.E. Baxter, eds., Standard Methods for the Examination of Water and Wastewater, 24th ed., APHA Press, Washington DC, 2023. https://doi.org/10.4269/ajtmh.1940.s1-20.459.

[26] P.L. Searle, The berthelot or indophenol reaction and its use in the analytical chemistry of nitrogen: a review, Analyst 109 (1984) 549–568, https://doi.org/10.1039/AN9840900549.

[27] N.A. Sacco, F. Miranda Zoppas, V. Aghemo, T. Beltrame, F.A. Marchesini, Pd/In-based catalysts for nitrate catalytic removal from water: synthesis designs aiming for better N2 selectivity, Water Supp 23 (2023) 526–545, https://doi.org/10.2166/ws.2023.019.

[28] F.A. Marchesini, S. Irusta, C. Querini, E. Miró, Nitrate hydrogenation over Pt,In/Al2O3 and Pt,In/SiO2. Effect of aqueous media and catalyst surface properties upon the catalytic activity, Catal. Commun. 9 (2008) 1021–1026, https://doi.org/10.1016/j.catcom.2007.09.037.

[29] I. Patiha, Maulidan Firdaus (Sebelas Maret University, Review and improved technique of the initial rate method, Chem.: Bulg. J. Sci. Educ. 28 (2019) 34–47.

[30] J. Casado, M.A. López-Quintela, F.M. Lorenzo-Barral, The initial rate method in chemical kinetics: evaluation and experimental illustration, J. Chem. Educ. 63 (1986) 450–452, https://doi.org/10.1021/ed063p450.

[31] M. Ribota Peláez, E. Ruiz-López, M.I. Domínguez, S. Ivanova, M.A. Centeno, Formic acid dehydrogenation over a monometallic Pd and bimetallic Pd:Co catalyst supported on activated carbon, Catalysts 13 (2023), https://doi.org/10.3390/catal13060977.

[32] E.S. Osipova, D.V. Sedlova, E.I. Gutsul, Y.V. Nelyubina, P.V. Dorovatovskii, L. M. Epstein, O.A. Filippov, E.S. Shubina, N.V. Belkova, Reactivity of heterobimetallic ion pairs in formic acid dehydrogenation, Organometallics 42 (2023) 2651–2660, https://doi.org/10.1021/acs.organomet.3c00125.

[33] M. Karatok, H.T. Ngan, X. Jia, C.R. O'Connor, J.A. Boscoboinik, D.J. Stacchiola, P. Sautet, R.J. Madix, Achieving ultra-high selectivity to hydrogen production from formic acid on Pd-Ag alloys, J. Am. Chem. Soc. 145 (2023) 5114–5124, https://doi.org/10.1021/jacs.2c11323.

[34] A. Dong, Q. Jiang, Y. Zhou, Au3Pd1 intermetallic compound as single atom catalyst for formic acid decomposition with highly hydrogen selectivity, Int J. Hydrog. Energy 48 (2023) 29542–29551, https://doi.org/10.1016/J.IJHYDENE.2023.04.113.

[35] A. Garron, F. Epron, Use of formic acid as reducing agent for application in catalytic reduction of nitrate in water, Water Res 29 (2005) 3073.

[36] S. Bhandari, S. Rangarajan, S. Li, J. Scaranto, S. Singh, C.T. Maravelias, J. A. Dumesic, M. Mavrikakis, A coverage self-consistent microkinetic model for vapor-phase formic acid decomposition over Pd/C catalysts, ACS Catal. 13 (2023) 3655–3667, https://doi.org/10.1021/acscatal.2c06078.

[37] Z. Dou, L. Wang, J. Hu, W. Fang, C. Sun, Z. Men, Hydrogen bonding effect on Raman modes of Formic acid-water binary solutions, J. Mol. Liq. 313 (2020) 113595, https://doi.org/10.1016/J.MOLLIQ.2020.113595.

[38] A. Bende, M.F. Gaele, T.M. Di Palma, Photoionization, structures, and energetics of Na-doped formic acid–water clusters, ChemPhysChem 23 (2022), https://doi.org/10.1002/cphc.202100861.

[39] A. Pintar, Catalytic processes for the purification of drinking water and industrial effluents, Catal. Today 77 (2003) 451–465, https://doi.org/10.1016/S0920-5861(02)00385-1.

[40] A. Pintar, J. Batista, Improvement of an integrated ion-exchange/catalytic process for nitrate removal by introducing a two-stage denitrification step, Appl. Catal., B 63 (2006) 150.

[41] Y. Sakamoto, M. Kanno, T. Okuhara, Y. Kamiya, Highly selective hydrogenation of nitrate to harmless compounds in water over copper–palladium bimetallic clusters supported on active carbon, Catal. Lett. 125 (2008) 392–395, https://doi.org/10.1007/s10562-008-9574-6.

[42] H. jin Jeon, Y.M. Chung, Hydrogen production from formic acid dehydrogenation over Pd/C catalysts: effect of metal and support properties on the catalytic performance, Appl. Catal. B 210 (2017) 212–222, https://doi.org/10.1016/j.apcatb.2017.03.070.

[43] P. Xu, S. Agarwal, L. Lefferts, Mechanism of nitrite hydrogenation over Pd/γ-Al2O3 according a rigorous kinetic study, J. Catal. 383 (2020) 124–134, https://doi.org/10.1016/j.jcat.2020.01.003.

[44] U. Prüsse, K.D. Vorlop, Supported bimetallic palladium catalysts for water-phase nitrate reduction, J. Mol. Catal. A Chem. 173 (2001) 313–328, https://doi.org/10.1016/S1381-1169(01)00156-X.

[45] Y. Tang, C.A. Roberts, R.T. Perkins, I.E. Wachs, Revisiting formic acid decomposition on metallic powder catalysts: exploding the HCOOH decomposition volcano curve, Surf. Sci. 650 (2016) 103–110, https://doi.org/10.1016/j.susc.2015.12.032.

[46] L.L. Jewell, B.H. Davis, Review of absorption and adsorption in the hydrogen-palladium system, Appl. Catal. A Gen. 310 (2006) 1–15, https://doi.org/10.1016/j.apcata.2006.05.012.

[47] D. Vardanega, S. Picaud, Water and formic acid aggregates: a molecular dynamics study, J. Chem. Phys. 141 (2014), https://doi.org/10.1063/1.4894658.

[48] R.S. Postma, R. Brunet Espinosa, L. Lefferts, Competitive adsorption of nitrite and hydrogen on palladium during nitrite hydrogenation, ChemCatChem 10 (2018) 3770–3776, https://doi.org/10.1002/cctc.201800523.

[49] N.A. Sacco, F.M. Zoppas, T.F. Beltrame, E.E. Miró, F.A. Marchesini, Interference effects of oxyanions commonly found in natural waters on the catalytic reduction of nitrate in water, Environ. Sci. Pollut. Res 30 (2023) 37462–37474, https://doi.org/10.1007/s11356-022-24909-2.

[50] E. kyoung Choi, K. hyun Park, H. bin Lee, M. Cho, S. Ahn, Formic acid as an alternative reducing agent for the catalytic nitrate reduction in aqueous media, J. Environ. Sci. (China) 25 (2013) 1696–1702, https://doi.org/10.1016/S1001-0742(12)60226-5.

[51] K.E. Daumit, A.J. Carrasquillo, R.A. Sugrue, J.H. Kroll, Effects of condensed-phase oxidants on secondary organic aerosol formation, J. Phys. Chem. A 120 (2016) 1386–1394, https://doi.org/10.1021/acs.jpca.5b06160.

[52] V.N. Kalevaru, A. Benhmid, J. Radnik, M.M. Pohl, U. Bentrup, A. Martin, Marked influence of support on the catalytic performance of PdSb acetoxylation catalysts: Effects of Pd particle size, valence states, and acidity characteristics, J. Catal. 246 (2007) 399–412, https://doi.org/10.1016/J.JCAT.2007.01.002.